

GENERALIZED SYNTHESIS AND DESIGN OF SYMMETRICAL MULTIPLE PASSBAND FILTERS

A. Mohan^{1, *}, S. Singh², and A. Biswas³

¹Center for Excellence in ICT, Indian Institute of Technology Rajasthan, Jodhpur 342011, India

²Space Applications Centre, Indian Space Research Organisation, Ahmedabad 308015, India

³Department of Electrical Engineering, Indian Institute of Technology, Kanpur 208016, India

Abstract—In this paper, we present a new synthesis method for a generalized symmetric multiple band bandpass filter. By using frequency transformations on the low pass prototype, the poles and zeros of the single/dual band filtering function are obtained. These poles and zeros are combined and re-arranged to get the multiband filtering function. The coupling matrix is obtained from this multiband filtering function. A variety of filters are synthesized in order to validate the proposed theory. A triple band and quadruple band filters have been designed, fabricated and measured. The measured results have good agreement with the simulated results.

1. INTRODUCTION

In modern microwave communication systems one frequently requires a complex arrangement of frequency plans that have spatial coverage. Non-contiguous channels might need to be amplified and transmitted through a single beam. Multiple pass band filters can make the system simpler in comparison to the power divider/combiner configuration and circulator chain structures. For applications in satellite communication, dual-pass band elliptic waveguide filters of in-line type and canonical type have been reported [1, 2]. In case of cellular radio communication systems, dual bandpass filters of a canonical structure with a single mode technique have been designed

Received 16 April 2012, Accepted 1 July 2012, Scheduled 2 July 2012

* Corresponding author: Akhilesh Mohan (am@iitj.ac.in).

and realized [3]. In [4], triple and quad band bandpass filters based on lumped-element coplanar waveguide resonators are designed. It uses the concept of multiband resonator.

The multiband bandpass filter is realized by either placing transmission zeros within the passband of a wideband filter or employing higher order resonances [5,6]. In [7,8], an equivalent lumped network is introduced in order to achieve the multiband filtering. This network simplified the design procedure for dual band or multiband filters through iterative method. The problems such as need for optimization for roots finding and inability to achieve equiripple response occurred while applying the equivalent networks. Also, the optimization techniques might end up at a local minimum and they have poor rate of convergence, i.e., they require more number of iterations to obtain a reasonable convergence. Such problems can be minimized if the frequency transformation method is used for the design of multiband filters.

In [9–13], the multiband bandpass filters based on frequency transformation have been investigated. The complexity of the frequency transformation increases with the number of passband in multiband bandpass filters. A complex frequency transformation is required for the triple band bandpass filter [11]. In order to obtain a frequency response having multiple passbands, a new network called multiband block concept is proposed [13]. A multiband block uses the frequency mapping. The multiband block is formed by the connection of n resonators, where n is the number of passbands in the filter. In multiband block, one of the resonator is the original single band resonator, while the additional resonators are coupled to the original resonator through couplings or admittance inverters. As the number of passbands in the multiband filter increases, the number of coupling coefficients from original single resonator to other resonators increases. Therefore, it is very difficult when it comes to hardware implementation.

Another frequency transformation based multiband filter design has been discussed [12]. The response of the multiband filter is generated via the proper combination of the single-band filtering functions; those single band filtering functions can be obtained by using Cameron's advanced coupling matrix synthesis technique [14]. In case of symmetrical dual band filter, the multiband filter response can be generated by properly combining two single band frequency responses. Additional transmission zero at 0 rad/s is introduced to meet the phase requirement of two single band filtering functions.

In this paper, an analytical method is proposed for the synthesis of symmetrical multiple passband filters. The multiband filter response

is generated from the multiband filtering function. The frequency transformations have been used for transforming the lowpass prototype to the required multiband configuration. The proposed method simplifies the generalized synthesis of symmetrical multiple passband filters. This multiband filtering function is generated by combining the poles and zeros of single/dual band filtering function obtained by the frequency transformation method. Different methods are proposed for the filters having even and odd number of passbands. In case of multiple band filter having even number of passbands, the overall filter response is divided into $M = N/2$ number of dual passbands. The filtering function for these M dual passbands are evaluated and are combined together to form a multiband filtering function. The poles and zeros of M dual passbands are used for the construction of multiband filtering function. Once the poles and zeros of the multiband filtering function are known, one can obtain the fractional forms of the scattering parameters in terms of the $P_N(s)$, $F_N(s)$ and $E_N(s)$ polynomials. It is possible to obtain the transversal coupling matrix from these polynomials [14].

The transversal coupling matrix can be converted into wheel matrix using Bell's technique [15]. This wheel matrix can, in turn, be converted into multiband filter matrix with the desired coupling scheme for the hardware implementation. This desired coupling scheme can be either in canonical form or N -tuplets form.

The steps for the synthesis of multiple passband filters are discussed in Section 2. Sections 3 and 4 present the synthesis of filters having even and odd number of passbands. To verify the proposed method, a triple and a quad band bandpass filters are realized using the open loop resonators. The cascaded quadruplets are used for realizing the transmission zeros.

2. THEORY AND DESIGN PROCEDURE

In this section, we have introduced a procedure for designing multiple passband microwave filters using frequency transformations. The frequency responses for the filter having even number of pass bands in three different frequency domains are shown in Fig. 1. Ω -domain is the normalized frequency domain for the lowpass prototype filter, Ω' -domain is the intermediate frequency domain which is used design of multiple passband filters, whereas ω -domain is the actual frequency domain in which the filter operates.

The transfer and reflection functions for any two port lossless filter network consisting of a series of N -coupled resonators can be expressed

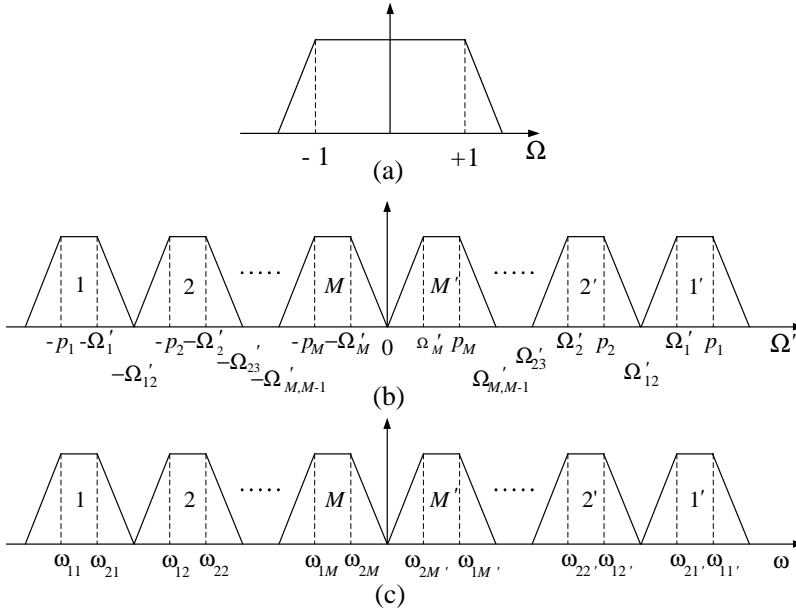


Figure 1. (a) Low-pass prototype response. The frequency response of the filter having an even number of the passband in (b) Ω' and (c) ω -domain.

as [14]:

$$S_{21}(S) = \frac{P_N(S)}{\varepsilon E_N(S)} \quad (1)$$

$$S_{11}(S) = \frac{F_N(S)}{E_N(S)} \quad (2)$$

where $S = j\Omega$. For a Chebyshev filtering function, ε is a constant normalizing S_{21} to the equi-ripple level at $S = \pm j$ as follows:

$$\varepsilon = \frac{1}{\sqrt{10^{RL/10} - 1}} \left. \frac{P_N(S)}{F_N(S)} \right|_{S=j} \quad (3)$$

where RL is the prescribed return loss level in dB and it is assumed that all the polynomials have been normalized such that their highest degree coefficients are unity. Once P_N and F_N are defined, the unitary condition of S -parameter requires that

$$E_N(S) E_N^*(-S) = \frac{P_N(S) P_N^*(-S)}{\varepsilon^2} + F_N(S) F_N^*(-S) \quad (4)$$

where $E_N^*(S)$, $P_N^*(S)$ and $F_N^*(S)$ denotes the complex conjugate of $E_N(S)$, $P_N(S)$ and $F_N(S)$ respectively.

The poles of $S_{11}(S)$ or $S_{21}(S)$ can be obtained by evaluating the roots of the Equation (4) and by selecting those having the negative real part. Again, here $E_N(s)$ is generated from the poles of $S_{11}(S)$ or $S_{21}(S)$ by imposing the highest degree coefficient equal to unity.

Using Equations (1), (2) and (4), we get,

$$|S_{11}(S)|^2 = \frac{\varepsilon^2 C_N^2(S)}{1 + \varepsilon^2 C_N^2(S)} \quad (5)$$

$$|S_{21}(S)|^2 = \frac{1}{1 + \varepsilon^2 C_N^2(S)} \quad (6)$$

where $C_N(S) = \frac{F_N(S)}{P_N(S)}$ is known as the filtering function of degree N .

$P_N(S')$, $F_N(S')$, $E_N(S')$ and ε can be evaluated by using the poles and zeros of the multiband filtering function after the frequency transformation in Ω' -domain, where $S' = j\Omega'$. The coupling matrix for a given topology can be calculated using the polynomials $P_N(S')$, $F_N(S')$, $E_N(S')$ and ε by using Cameron's method [14]. The steps for building the coupling matrix are given below.

2.1. For Even Number of Passbands

Step 1: Choose the lowpass prototype as per the required attenuation in the stopband.

Step 2: Divide N passbands into M dual passbands where $M = N/2$. The dual passbands are paired as $(1, 1')$, $(2, 2')$, \dots , (M, M') . $(1, 1')$ represents the outermost passbands and (M, M') the innermost passbands as shown in Fig. 1(b).

Step 3: Transform the lowpass prototype filter to the outermost dual passbands $(1, 1')$. Also, transform the lowpass prototype filter to other dual passbands such as $(2, 2')$, \dots , (M, M') .

Step 4: Evaluate all the poles and zeros of filtering function for each frequency transformation in each of the dual passbands.

Step 5: Combine the poles and zeros of all the transformed functions for the construction of multiband filtering function.

Step 6: Remove the overlapped poles and rearrange the poles and zeros of the multiband filtering function using either optimization or error and trial method [16].

Step 7: Construct the polynomials P_N , F_N , E_N and ε in S' -plane using the poles and zeros of the multiband filtering function.

Step 8: Obtain the transversal coupling matrix from these polynomials [14].

Step 9: Convert the transversal coupling matrix into Bell's wheel matrix form [15].

Step 10: Generate the desired coupling matrix from wheel matrix for hardware implementation [17].

The frequency transformations from Ω -domain to Ω' -domain convert the lowpass prototype into normalized dual passband filter [10]. The frequency transformation is given as:

For $(1, 1')$ bands:

$$S = \left(\frac{S'}{c_1} + \frac{c'_1}{S'} \right) \quad \text{for } \Omega' > \Omega'_{12} \quad (7)$$

$$S = - \left(\frac{S'}{c_1} + \frac{c'_1}{S'} \right) \quad \text{for } \Omega' < -\Omega'_{12} \quad (8)$$

For $(2, 2')$ bands:

$$S = \left(\frac{S'}{c_2} + \frac{c'_2}{S'} \right) \quad \text{for } \Omega'_{23} < \Omega' < \Omega'_{12} \quad (9)$$

$$S = - \left(\frac{S'}{c_2} + \frac{c'_2}{S'} \right) \quad \text{for } -\Omega'_{12} < \Omega' < -\Omega'_{23} \quad (10)$$

For (M, M') bands:

$$S = \left(\frac{S'}{c_M} + \frac{c'_M}{S'} \right) \quad \text{for } 0 < \Omega' < \Omega'_{M,M-1} \quad (11)$$

$$S = - \left(\frac{S'}{c_M} + \frac{c'_M}{S'} \right) \quad \text{for } -\Omega'_{M,M-1} < \Omega' < 0 \quad (12)$$

where $S = j\Omega$ and $S' = j\Omega'$.

Since 1 and -1 in the Ω -domain are transformed to p_1 and Ω'_1 in the Ω' -domain for $\Omega' > \Omega'_{12}$, respectively, and 1 and -1 in the Ω -domain are transformed to $-p_1$ and $-\Omega'_1$ in Ω' -domain for $\Omega' < -\Omega'_{12}$, respectively. In order to carry out the transformations, we must enforce the following

$$p_1 = \frac{c_1}{2} \left(1 + \sqrt{1 + 4 \frac{c'_1}{c_1}} \right) \quad (13)$$

$$\Omega'_1 = \frac{c_1}{2} \left(-1 + \sqrt{1 + 4 \frac{c'_1}{c_1}} \right) \quad (14)$$

Similarly, for all the dual pass band pairs, we must enforce p 's and Ω' 's for calculating the constants c 's. From Equations (13) and (14), the constants in the Equations (7) and (8) can be expressed in terms of

the band edge frequencies of the first dual band pair in Ω' -domain as follows:

$$c_1 = p_1 - \Omega'_1, \quad c'_1 = \frac{p_1 \Omega'_1}{p_1 - \Omega'_1} \quad (15)$$

Similarly, other remaining constants can be expressed in Ω' -domain as follows:

$$c_2 = p_2 - \Omega'_2, \quad c'_2 = \frac{p_2 \Omega'_2}{p_2 - \Omega'_2} \quad (16)$$

...

$$c_M = p_M - \Omega'_M, \quad c'_M = \frac{p_M \Omega'_M}{p_M - \Omega'_M} \quad (17)$$

The band edge frequencies in the Ω' -domain to be transformed to the actual ω -domain are as follows:

$$\begin{aligned} p_1 &\rightarrow \omega_{11'} \\ \Omega'_1 &\rightarrow \omega_{21'} \\ p_2 &\rightarrow \omega_{12'} \\ \Omega'_2 &\rightarrow \omega_{22'} \\ &\dots \\ p_M &\rightarrow \omega_{1M'} \\ \Omega'_M &\rightarrow \omega_{2M'} \\ -\Omega'_M &\rightarrow \omega_{2M} \\ -p_M &\rightarrow \omega_{1M} \\ &\dots \\ -\Omega'_2 &\rightarrow \omega_{22} \\ -p_2 &\rightarrow \omega_{12} \\ -\Omega'_1 &\rightarrow \omega_{21} \\ -p_1 &\rightarrow \omega_{11} \end{aligned}$$

The values of $\omega_{11}, \omega_{21}, \omega_{11'}, \omega_{21'}, \dots$ can be expressed in terms of band edge frequencies in Ω' -domain.

The transformation used for Ω' -domain to ω -domain for the outermost dual passbands (1, 1') is

$$S' = \left(\frac{s}{d_1} + \frac{d'_1}{s} \right) \quad (18)$$

Similarly, for the (2, 2') dual passbands, the transformation is

$$S' = \left(\frac{s}{d_2} + \frac{d'_2}{s} \right) \quad (19)$$

For (M, M') dual passbands, the transformation is

$$S' = \left(\frac{s}{d_M} + \frac{d'_M}{s} \right) \quad (20)$$

where $s = j\omega$.

The values of d_1 and d'_1 are as follows:

$$d_1 = \frac{\omega_{11'} - \omega_{11}}{p_1}, \quad d'_1 = \frac{\omega_{11}\omega_{11'}}{\omega_{11'} - \omega_{11}} p_1 \quad (21)$$

and similarly the other values of d 's are

$$d_2 = \frac{\omega_{21'} - \omega_{21}}{p_2}, \quad d'_2 = \frac{\omega_{21}\omega_{21'}}{\omega_{21'} - \omega_{21}} p_2 \quad (22)$$

$$\dots$$

$$d_M = \frac{\omega_{M1'} - \omega_{M1}}{p_M}, \quad d'_M = \frac{\omega_{M1}\omega_{M1'}}{\omega_{M1'} - \omega_{M1}} p_M \quad (23)$$

2.2. For Odd Number of Passbands

In this section, the synthesis method for the design of multiple band bandpass filters having odd number of pass bands is discussed.

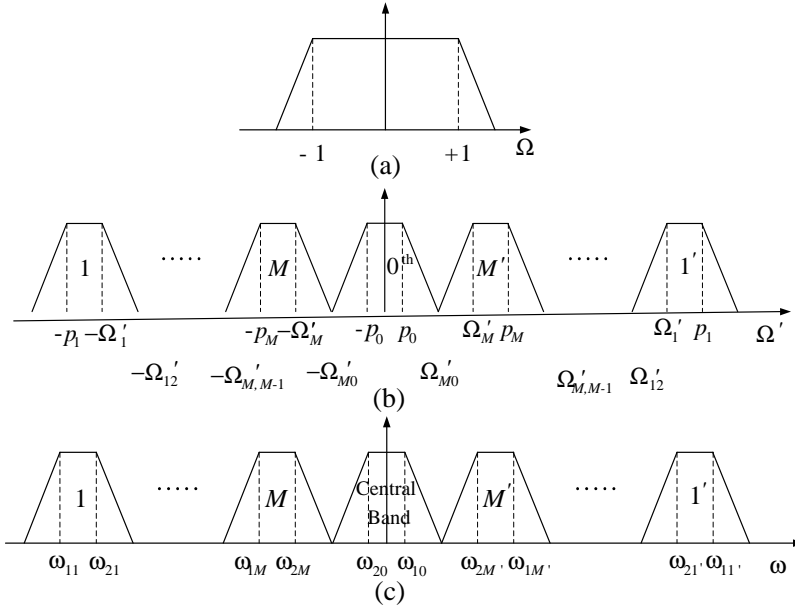


Figure 2. (a) Low-pass prototype response. The frequency response of the filter having an odd number of passband in (b) Ω' and (c) ω -domain.

Step 1: Choose the lowpass prototype as per required attenuation in the stopband.

Step 2: Divide the N -passbands into $2M + 1$ discrete passbands where M is the number of dual-passbands. The dual passbands are designated in pairs as $(1, 1')$, $(2, 2')$, ..., (M, M') and the single passband as 0th or central passband as shown in Fig. 2.

Step 3: Transform the lowpass prototype filter to dual bandpass filters $(1, 1')$, $(2, 2')$, ..., (M, M') using similar frequency transformations discussed earlier. Also, transform the lowpass prototype to the central passband.

Steps from 4 to 10 are the same as that of even number of passbands.

The transformation for the central passband is given as

$$S = \left(\frac{S'}{c_0} \right) \quad \text{for} \quad -p_0 < \Omega' < p_0 \quad (24)$$

where $c_0 = p_0$.

The frequency transformations from Ω' -domain to ω -domain for dual passband pairs discussed in the context of even number of passbands hold good in the present case. The transformation for central passband is given as:

$$S' = \left(\frac{s}{d_0} \right) \quad (25)$$

where $s = j\omega$.

The additional band edge frequencies in the Ω' -domain to be transformed to the actual ω -domain are as follows:

$$\begin{aligned} p_0 &\rightarrow \omega_{10} \\ -p_0 &\rightarrow \omega_{20} \end{aligned}$$

3. SYMMETRICAL EVEN NUMBER OF PASSBAND FILTER SYNTHESIS

In this section a 16-pole quadruple band and 24-pole hexa band bandpass filters are synthesized in order to validate the present approach of filter synthesis.

3.1. A 16-pole Quadruple Band Bandpass Filter

In order to get a four pole passband response in each passband a four pole lowpass prototype with finite transmission zeros at $S = \pm j2.0$ is chosen for synthesis. The location of the transmission zeros depends upon the attenuation requirement over the stopband. The reflection

zeros of the filter can be calculated using the process described in [18] according to the specified transmission zeros, return loss and number of poles. In order to synthesize a symmetrical quadruple band bandpass filter we have chosen $p_1 = 1$, $\Omega'_1 = 0.80$, $p_2 = 0.40$, $\Omega'_2 = 0.20$ and the corresponding values of c 's are $c_1 = 0.20$, $c'_1 = 4.0$, $c_2 = 0.20$ and $c'_2 = 0.40$. After using all the transformations described in the Section 2.1, the final poles and zeros of the multiband filtering functions are obtained and they are presented in Table 1.

As has been discussed in the Section 2.1, the next step in synthesis is the removal of the overlapped transmission zeros (poles of multiband filtering function). The removal of transmission zeros may disturb the frequency response of the filter. To preserve the desired frequency response, some additional transmission zeros may be introduced and the poles and zeros of the filtering function are rearranged. But, here

Table 1. Poles and zeros of quad band filtering function.

| Poles | Zeros |
|---------------|---------------|
| $\pm j1.1165$ | $\pm j0.9926$ |
| $\pm j0.7165$ | $\pm j0.9360$ |
| $\pm j0.5464$ | $\pm j0.8547$ |
| $\pm j0.1464$ | $\pm j0.8060$ |
| $\pm j0$ | $\pm j0.3912$ |
| $\pm j0$ | $\pm j0.3263$ |
| | $\pm j0.2451$ |
| | $\pm j0.2045$ |

Table 2. Poles and zeros of quad band filtering function after removal of overlapped TZs and rearrangement.

| Poles | Zeros |
|---------------|---------------|
| $\pm j1.1165$ | $\pm j0.9926$ |
| $\pm j0.7165$ | $\pm j0.9360$ |
| $\pm j0.6410$ | $\pm j0.8547$ |
| $\pm j0.5464$ | $\pm j0.8060$ |
| $\pm j0.1464$ | $\pm j0.3912$ |
| $\pm j0$ | $\pm j0.3263$ |
| | $\pm j0.2451$ |
| | $\pm j0.2045$ |

in this case, the removal of poles at $\pm j0$ and addition of poles at $\pm j0.6410$ do not disturb the response. That means, the frequency response remains the same. The poles and zeros of the multiband filtering function after the rearrangement are given in Table 2. The polynomials F_N , P_N , E_N and ε can be constructed using the poles and zeros of the multiband filtering function. The coefficients of the polynomials are shown in Table 3.

Table 3. 16-pole symmetric quad-band bandpass filter: coefficients of transfer and reflection polynomials.

| s^n $n =$ | P_N | F_N | E_N |
|-------------|--------|-----------|-----------|
| 0 | 0 | $1.67e-5$ | $1.67e-5$ |
| 1 | 0 | 0 | $9.79e-5$ |
| 2 | 0.0017 | 0.0010 | 0.0013 |
| 3 | 0 | 0 | 0.0052 |
| 4 | 0.0926 | 0.0235 | 0.0340 |
| 5 | 0 | 0 | 0.0890 |
| 6 | 0.7115 | 0.2511 | 0.3633 |
| 7 | 0 | 0 | 0.6303 |
| 8 | 2.0615 | 1.3437 | 1.8326 |
| 9 | 0 | 0 | 2.0867 |
| 10 | 2.4895 | 3.6355 | 4.6416 |
| 11 | 0 | 0 | 3.4432 |
| 12 | 1 | 5.1234 | 6.0950 |
| 13 | | 0 | 2.7441 |
| 14 | | 3.6029 | 3.9559 |
| 15 | | 0 | 0.8402 |
| 16 | | 1 | 1 |

and $\varepsilon = 41.57$.

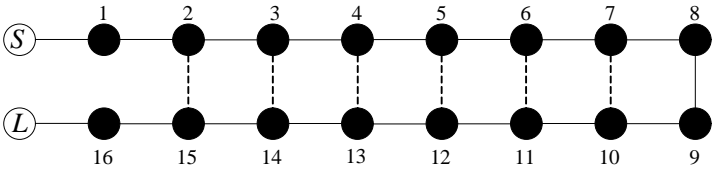


Figure 3. Canonical topology of Quadruple band bandpass filter.

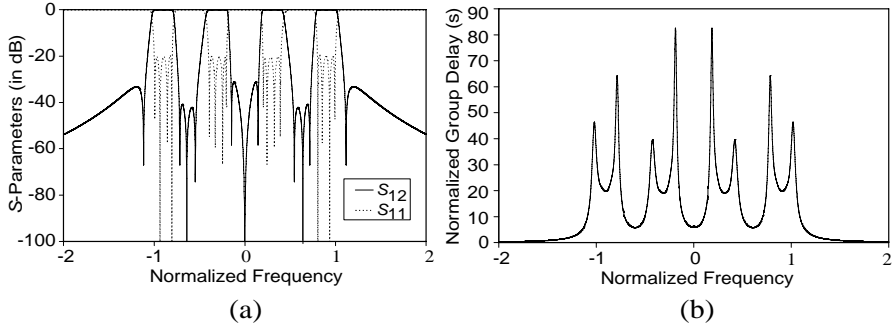


Figure 4. Frequency response of a 16 pole quadruple passband. (a) S -parameters. (b) Group delay.

From the polynomials F_N , P_N , E_N and ε , the coupling matrix of the canonical prototype filter, shown in Fig. 3, is obtained.

The coupling matrix is given of quadruple band bandpass filter is given as:

$$M = \begin{bmatrix} 0 & 0.6481 & 0 & 0 & 0 & 0 & 0 & 0 & 0 & 0 & 0 & 0 & 0 & 0 & 0 & 0 & 0 \\ 0.6481 & 0 & 0.7164 & 0 & 0 & 0 & 0 & 0 & 0 & 0 & 0 & 0 & 0 & 0 & 0 & 0 & 0 \\ 0 & 0.7164 & 0 & 0.5647 & 0 & 0 & 0 & 0 & 0 & 0 & 0 & 0 & 0 & 0 & 0 & -0.0558 & 0 \\ 0 & 0 & 0.5647 & 0 & 0.4767 & 0 & 0 & 0 & 0 & 0 & 0 & 0 & 0 & 0 & 0.0661 & 0 & 0 \\ 0 & 0 & 0 & 0.4767 & 0 & -0.4246 & 0 & 0 & 0 & 0 & 0 & 0 & 0 & -0.0796 & 0 & 0 & 0 \\ 0 & 0 & 0 & 0 & -0.4246 & 0 & 0.6402 & 0 & 0 & 0 & 0 & 0 & 0.2588 & 0 & 0 & 0 & 0 \\ 0 & 0 & 0 & 0 & 0 & 0.6402 & 0 & 0.2872 & 0 & 0 & -0.1070 & 0 & 0 & 0 & 0 & 0 & 0 \\ 0 & 0 & 0 & 0 & 0 & 0 & 0.2872 & 0 & -0.2814 & 0 & 0.2543 & 0 & 0 & 0 & 0 & 0 & 0 \\ 0 & 0 & 0 & 0 & 0 & 0 & 0 & -0.2814 & 0 & 0.0097 & 0 & 0 & 0 & 0 & 0 & 0 & 0 \\ 0 & 0 & 0 & 0 & 0 & 0 & 0 & 0 & 0.0097 & 0 & 0.2814 & 0 & 0 & 0 & 0 & 0 & 0 \\ 0 & 0 & 0 & 0 & 0 & 0 & 0 & 0.2543 & 0 & 0.2814 & 0 & -0.2872 & 0 & 0 & 0 & 0 & 0 \\ 0 & 0 & 0 & 0 & 0 & 0 & -0.1070 & 0 & 0 & 0 & -0.2872 & 0 & 0.6402 & 0 & 0 & 0 & 0 \\ 0 & 0 & 0 & 0 & 0 & 0.2588 & 0 & 0 & 0 & 0 & 0 & 0.6402 & 0 & 0.4246 & 0 & 0 & 0 \\ 0 & 0 & 0 & 0 & -0.0796 & 0 & 0 & 0 & 0 & 0 & 0 & 0 & 0.4246 & 0 & 0.4767 & 0 & 0 \\ 0 & 0 & 0 & 0.0661 & 0 & 0 & 0 & 0 & 0 & 0 & 0 & 0 & 0 & -0.4767 & 0 & 0.5647 & 0 \\ 0 & 0 & -0.0558 & 0 & 0 & 0 & 0 & 0 & 0 & 0 & 0 & 0 & 0 & 0 & 0.5647 & 0 & 0.7064 \\ 0 & 0 & 0 & 0 & 0 & 0 & 0 & 0 & 0 & 0 & 0 & 0 & 0 & 0 & 0 & 0.7164 & 0.6481 \\ 0 & 0 & 0 & 0 & 0 & 0 & 0 & 0 & 0 & 0 & 0 & 0 & 0 & 0 & 0 & 0.6481 & 0 \end{bmatrix}$$

The frequency response and normalized group delay response of the quadruple band bandpass filter are shown in Fig. 4(a) and Fig. 4(b) respectively. It is clear from Fig. 4(a) that the stopband attenuation between the passbands is 30 dB. The quadruple band bandpass filter has an equi-ripple response in the passbands and the return loss of each passband is 20 dB.

3.2. A 24-pole Hexa Band Bandpass Filter

Since the requirement is to get a four pole passband response, a four pole lowpass prototype is chosen. A pair of transmission zeros are located at $s = \pm j2.0$ and return loss is set to be 20 dB. The reflection zeros are computed as $s = \pm j0.9333$ and $s = \pm j0.4060$. We have chosen $p_1 = 1.0$, $\Omega'_1 = 0.875$, $p_2 = 0.625$, $\Omega'_2 = 0.5$, $p_3 = 0.25$, $\Omega'_3 = 0.125$ in order to synthesize a symmetrical hexa band filter response. The corresponding values of c 's are $c_1 = 0.125$, $c'_1 = 7$, $c_2 = 0.125$, $c'_2 = 2.5$, $c_3 = 0.125$, $c'_3 = 0.25$. Using the frequency transformation described in Section 2.1, the poles and zeros of the multiband filtering function in Ω' -domain are obtained and they are presented in Table 4.

There are three pairs of repeated transmission zeros at $\pm j0$. We can remove two such pairs of transmission zeros. In order to preserve the frequency response, some new transmission zeros can be introduced. In this synthesis, $\pm j0.7610$ and $\pm j0.4027$ are the new transmission zeros introduced in the multiband filtering response. The introduction of new transmission zeros will require re-arrangement of poles and zeros of the filtering function. The poles and zeros of filtering function can be rearranged either optimization method [16] or by error trial method. We have used error and trial method for rearranging the poles and zeros. The rearranged poles and zeros of the filtering function are shown in Table 5. The polynomials F_N , P_N , E_N and ε can be obtained using the poles and zeros of the filtering function. The coefficients of the polynomials are shown in Table 6. From the

Table 4. Poles and zeros of Hexa band filtering function.

| Poles | Zeros |
|---------------|---------------|
| $\pm j0$ | $\pm j0.9956$ |
| $\pm j0$ | $\pm j0.9611$ |
| $\pm j0$ | $\pm j0.9104$ |
| $\pm j1.0687$ | $\pm j0.8789$ |
| $\pm j0.8187$ | $\pm j0.6204$ |
| $\pm j0.6978$ | $\pm j0.5850$ |
| $\pm j0.4478$ | $\pm j0.5342$ |
| $\pm j0.3415$ | $\pm j0.5037$ |
| $\pm j0.0915$ | $\pm j0.2445$ |
| | $\pm j0.2040$ |
| | $\pm j0.1532$ |
| | $\pm j0.1278$ |

Table 5. Poles and zeros of Hexa band filtering function after rearrangement.

| Poles | Zeros |
|---------------|---------------|
| $\pm j0$ | $\pm j0.9956$ |
| $\pm j1.0687$ | $\pm j0.9620$ |
| $\pm j0.8187$ | $\pm j0.9104$ |
| $\pm j0.7610$ | $\pm j0.8783$ |
| $\pm j0.6978$ | $\pm j0.6204$ |
| $\pm j0.4478$ | $\pm j0.5850$ |
| $\pm j0.4027$ | $\pm j0.5342$ |
| $\pm j0.3415$ | $\pm j0.5037$ |
| $\pm j0.0915$ | $\pm j0.2445$ |
| | $\pm j0.2040$ |
| | $\pm j0.1532$ |
| | $\pm j0.1278$ |

Table 6. 24-pole symmetric Hexa-band bandpass filter: Coefficients of transfer and reflection polynomials.

| $s^n \ n =$ | P_N | F_N | E_N |
|-------------|-----------|-----------|-----------|
| 0 | 0 | $5.3e-9$ | $5.33e-9$ |
| 1 | 0 | 0 | $6.17e-8$ |
| 2 | $6.85e-6$ | $8.65e-7$ | $1.22e-6$ |
| 3 | 0 | 0 | $9.2e-6$ |
| 4 | 0.0010 | 0.0001 | 0.0001 |
| 5 | 0 | 0 | 0.0004 |
| 6 | 0.0230 | 0.0016 | 0.0027 |
| 7 | 0 | 0 | 0.0094 |
| 8 | 0.2231 | 0.0249 | 0.0418 |
| 9 | 0 | 0 | 0.1031 |
| 10 | 1.1105 | 0.2222 | 0.3536 |
| 11 | 0 | 0 | 0.6484 |
| 12 | 3.0112 | 1.1950 | 1.7973 |
| 13 | 0 | 0 | 2.4910 |
| 14 | 4.4619 | 4.0455 | 5.7361 |
| 15 | 0 | 0 | 6.0024 |
| 16 | 3.3660 | 8.7855 | 11.7066 |
| 17 | 0 | 0 | 9.0665 |
| 18 | 1 | 12.1671 | 15.1853 |
| 19 | | 0 | 8.3025 |
| 20 | | 10.3553 | 12.0602 |
| 21 | | 0 | 4.2007 |
| 22 | | 4.9243 | 5.3283 |
| 23 | | 0 | 0.8989 |
| 24 | | 1 | 1 |

and $\varepsilon = 124.7609$.

polynomials F_N , P_N , E_N and ε , the coupling matrix of the canonical prototype filter, shown in Fig. 5, is obtained.

The topology of the symmetrical hexa band bandpass filter is shown in Fig. 5. The cross couplings are present in addition to inline coupling for the realization of the transmission zeros. This hexa band bandpass filter has nine pairs of transmission zeros. The synthesized frequency response of the hexa band bandpass filter is shown in Fig. 6. The return loss in some of the passbands is slightly greater than 20 dB.

4. SYMMETRICAL ODD NUMBER OF PASSBAND FILTER SYNTHESIS

In this section, synthesis of the multiple band bandpass filter having an odd number of passbands is presented.

4.1. A 12-pole Triple Band Bandpass filter

Here again, we have chosen the four pole lowpass prototype having transmission zeros at $S = \pm j2.0$. A symmetrical triple band response can be divided into a dual band and a single band response. The dual band response is in the outer bands of the triple band bandpass filter whereas the single band lies in the middle. We have chosen $p_1 = 1.0$, $\Omega'_1 = 0.60$, $p_0 = 0.20$ for the symmetrical triple band bandpass filter and the corresponding values of c 's are $c_1 = 0.40$, $c'_1 = 1.5$ and $c_0 = 0.2$. Using the frequency transformations, the poles and zeros of the dual band have been obtained and are given in Table 7. For

Table 7. Poles and zeros of outer dual band.

| Poles | Zeros |
|---------------|---------------|
| $\pm j1.2540$ | $\pm j0.9845$ |
| $\pm j0.4943$ | $\pm j0.8683$ |
| $\pm j0$ | $\pm j0.7140$ |
| | $\pm j0.6298$ |

Table 8. Poles and zeros of central single band.

| Poles | Zeros |
|-------------|---------------|
| $\pm j0.40$ | $\pm j0.1867$ |
| | $\pm j0.0812$ |

Table 9. Poles and zeros of triple band filtering function after rearrangement.

| Poles | Zeros |
|---------------|---------------|
| $\pm j1.5543$ | $\pm j0.9845$ |
| $\pm j0.4943$ | $\pm j0.8683$ |
| $\pm j0.3890$ | $\pm j0.7140$ |
| $\pm j0.3890$ | $\pm j0.6298$ |
| | $\pm j0.1867$ |
| | $\pm j0.0812$ |

Table 10. 12-pole symmetric triple-band bandpass filter: coefficients of transfer and reflection polynomials.

| $s^n \quad n =$ | P_N | F_N | E_N |
|-----------------|--------|----------|--------|
| 0 | 0.0135 | $3.4e-5$ | 0.0004 |
| 1 | 0 | 0 | 0.0038 |
| 2 | 0.2396 | 0.0064 | 0.0261 |
| 3 | 0 | 0 | 0.1135 |
| 4 | 1.4183 | 0.1902 | 0.4017 |
| 5 | 0 | 0 | 0.8593 |
| 6 | 2.9628 | 1.1149 | 1.9697 |
| 7 | 0 | 0 | 2.5020 |
| 8 | 1 | 2.6042 | 3.9888 |
| 9 | | 0 | 2.9828 |
| 10 | | 2.6711 | 3.4044 |
| 11 | | 0 | 1.2111 |
| 12 | | 1 | 1 |

and $\varepsilon = 36.0857$.

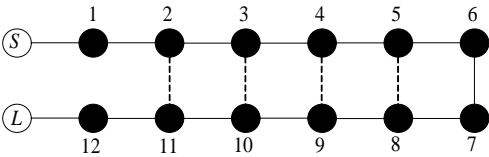


Figure 7. Canonical of triple band bandpass filter.

the single band also, the poles and zeros are obtained and are given in Table 8. Removing the transmission zeros present at the origin and rearranging the poles and zeros of the filtering function by error and trial method [16], we have obtained the desired triple pass band response shown in Fig. 8. The poles and zeros of the multiband filtering function after the rearrangement are given in Table 9. From these poles and zeros, the coefficients of the polynomials P_N , F_N , E_N and ε are calculated and are given in the Table 10. From the polynomials F_N , P_N , E_N and ε , the coupling matrix of the canonical prototype filter, shown in Fig. 7, is obtained.

The topology of the triple band bandpass filter is shown in Fig. 7. The frequency response of the 12-pole triple band bandpass filter and

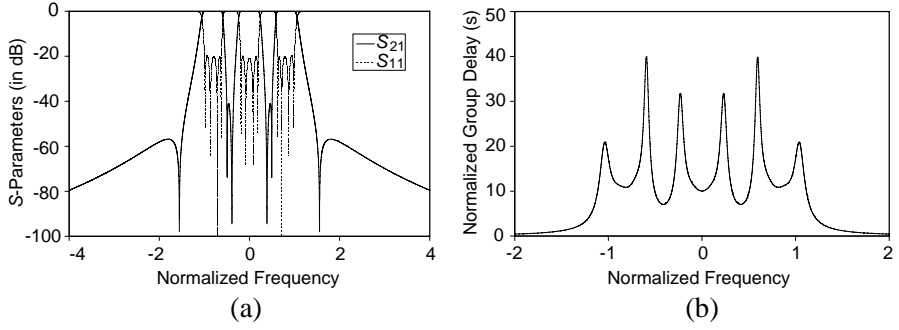


Figure 8. Frequency response of a 12 pole triple band bandpass filter. (a) S -parameters. (b) Group delay.

its normalized group delay is shown in Fig. 8.

The coupling matrix of 12-pole triple band bandpass filter is given as:

$$M = \begin{bmatrix} 0 & 0.7782 & 0 & 0 & 0 & 0 & 0 & 0 & 0 & 0 & 0 & 0 & 0 & 0 \\ 0.7782 & 0 & 0.7582 & 0 & 0 & 0 & 0 & 0 & 0 & 0 & 0 & 0 & 0 & 0 \\ 0 & 0.7582 & 0 & 0.5661 & 0 & 0 & 0 & 0 & 0 & 0 & 0 & -0.0398 & 0 & 0 \\ 0 & 0 & 0.5661 & 0 & 0.4388 & 0 & 0 & 0 & 0 & 0 & 0.2133 & 0 & 0 & 0 \\ 0 & 0 & 0 & 0.4388 & 0 & 0.5211 & 0 & 0 & 0 & 0.2523 & 0 & 0 & 0 & 0 \\ 0 & 0 & 0 & 0 & 0.5211 & 0 & 0.2485 & 0 & -0.0126 & 0 & 0 & 0 & 0 & 0 \\ 0 & 0 & 0 & 0 & 0 & 0.2485 & 0 & -0.2908 & 0 & 0 & 0 & 0 & 0 & 0 \\ 0 & 0 & 0 & 0 & 0 & 0 & -0.2908 & 0 & 0.2485 & 0 & 0 & 0 & 0 & 0 \\ 0 & 0 & 0 & 0 & 0 & -0.0126 & 0 & 0.2485 & 0 & 0.5211 & 0 & 0 & 0 & 0 \\ 0 & 0 & 0 & 0 & 0.2523 & 0 & 0 & 0 & 0.5211 & 0 & 0.4388 & 0 & 0 & 0 \\ 0 & 0 & 0 & 0.2133 & 0 & 0 & 0 & 0 & 0 & 0.4388 & 0 & 0.5661 & 0 & 0 \\ 0 & 0 & -0.0398 & 0 & 0 & 0 & 0 & 0 & 0 & 0 & 0.5661 & 0 & 0.7582 & 0 \\ 0 & 0 & 0 & 0 & 0 & 0 & 0 & 0 & 0 & 0 & 0 & 0.7582 & 0 & 0.7782 \\ 0 & 0 & 0 & 0 & 0 & 0 & 0 & 0 & 0 & 0 & 0 & 0 & 0.7782 & 0 \end{bmatrix}$$

5. REALIZATION OF MULTIBAND BANDPASS FILTERS

In order to verify the present approach, we have designed two multiple band bandpass filters: one triple band and one quadruple band bandpass filters. For the purpose of demonstration, we have removed the outer transmission zeros. This, in turn, reduces the number of cross couplings. The specifications of the triple band bandpass filter are as follows:

Center Frequency: 3.56 GHz

Overall Bandwidth: 400 MHz

Passband Return Loss > 20 dB

Using the synthesis method described in Section 2, the coupling matrix of the triple band bandpass filter is generated and is given below:

$$M = \begin{bmatrix} 0 & 0.8576 & 0 & 0 & 0 & 0 & 0 & 0 & 0 & 0 & 0 & 0 & 0 & 0 \\ 0.8576 & 0 & 0.7801 & 0 & 0 & 0 & 0 & 0 & 0 & 0 & 0 & 0 & 0 & 0 \\ 0 & 0.7801 & 0 & 0.5738 & 0 & 0 & 0 & 0 & 0 & 0 & 0 & 0 & 0 & 0 \\ 0 & 0 & 0.5738 & 0 & 0.4987 & 0 & 0 & 0 & 0 & 0 & 0 & 0 & 0 & 0 \\ 0 & 0 & 0 & 0.4987 & 0 & 0.4695 & 0 & -0.4016 & 0 & 0 & 0 & 0 & 0 & 0 \\ 0 & 0 & 0 & 0 & 0.4695 & 0 & 0.3449 & 0 & 0 & 0 & 0 & 0 & 0 & 0 \\ 0 & 0 & 0 & 0 & 0 & 0.3449 & 0 & 0.1516 & 0 & 0 & 0 & 0 & 0 & 0 \\ 0 & 0 & 0 & 0 & -0.4016 & 0 & 0.1516 & 0 & 0.6727 & 0 & 0 & 0 & 0 & 0 \\ 0 & 0 & 0 & 0 & 0 & 0 & 0 & 0.6727 & 0 & 0.2166 & 0 & -0.4253 & 0 & 0 \\ 0 & 0 & 0 & 0 & 0 & 0 & 0 & 0 & 0.2166 & 0 & 0.2548 & 0 & 0 & 0 \\ 0 & 0 & 0 & 0 & 0 & 0 & 0 & 0 & 0 & 0.2548 & 0 & 0.3851 & 0 & 0 \\ 0 & 0 & 0 & 0 & 0 & 0 & 0 & 0 & -0.4253 & 0 & 0.3851 & 0 & 0.7801 & 0 \\ 0 & 0 & 0 & 0 & 0 & 0 & 0 & 0 & 0 & 0 & 0 & 0.7801 & 0 & 0.8576 \\ 0 & 0 & 0 & 0 & 0 & 0 & 0 & 0 & 0 & 0 & 0 & 0 & 0.8576 & 0 \end{bmatrix}$$

This 12-pole triple band bandpass filter is realized using open loop microstrip resonators. The coupling topology, shown in Fig. 9, has cascaded quadruplets (CQ) structures. Each CQ structure realizes a pair of transmission zeros. The physical dimensions of the filter are calculated using the group delay method [19]. The finite Q -factor of the open loop resonator has been incorporated in the design of the filter

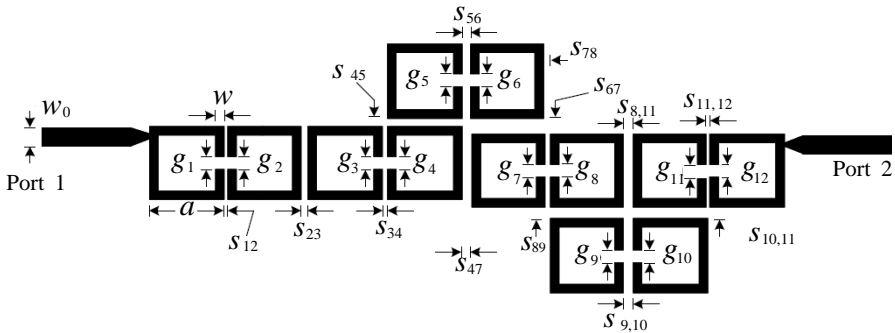


Figure 9. Layout of triple band bandpass filter. The filter physical dimensions are: $a = 9.71$ mm, $g_1 = 1.58$ mm, $g_2 = 1.72$ mm, $g_3 = 1.42$ mm, $g_4 = 1.56$ mm, $g_5 = 1.56$ mm, $g_6 = 1.6$ mm, $g_7 = 1.56$ mm, $g_8 = 1.56$ mm, $g_9 = 1.54$ mm, $g_{10} = 1.56$ mm, $g_{11} = 1.72$ mm, $g_{12} = 1.58$ mm, $s_{12} = 0.37$ mm, $s_{23} = 0.7$ mm, $s_{34} = 0.71$ mm, $s_{45} = 1.03$ mm, $s_{56} = 0.9$ mm, $s_{67} = 2.08$ mm, $s_{78} = 0.45$ mm, $s_{89} = 1.38$ mm, $s_{9,10} = 1.15$ mm, $s_{10,11} = 1.38$ mm, $s_{11,12} = 0.37$ mm, $s_{47} = 1.1$ mm, $s_{8,11} = 1.01$ mm.

($Q = 240$). Open loop resonator has been chosen because it provides electric, magnetic and mixed couplings and these couplings can be used for realizing both negative as well as positive couplings [20]. This filter is fabricated on the RT Duroid 5880 substrate which is having the dielectric constant of 2.2 and substrate thickness of 0.787 mm. The photograph of the fabricated triple band bandpass filter is shown in Fig. 10(a). The frequency response of the filter is synthesized using Agilent ADS and is shown in Fig. 10(b). During this synthesis, the finite Q -factor of the resonator is taken as 240. The chemical etching method is used for the fabrication of the filter. The full wave EM-simulator Agilent Momentum has been used for the design of the filter. The frequency response of the filter is measured on Agilent PNA

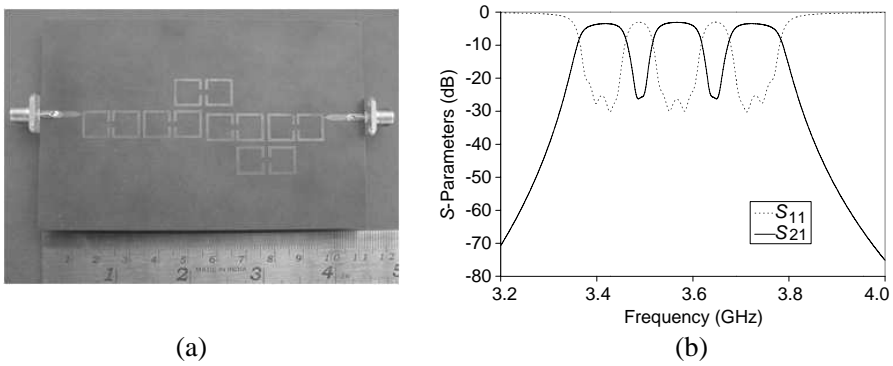


Figure 10. (a) Fabricated triple band bandpass filter. (b) Synthesized frequency response of triple band bandpass filter considering the finite Q -factor of the resonator $Q = 240$.

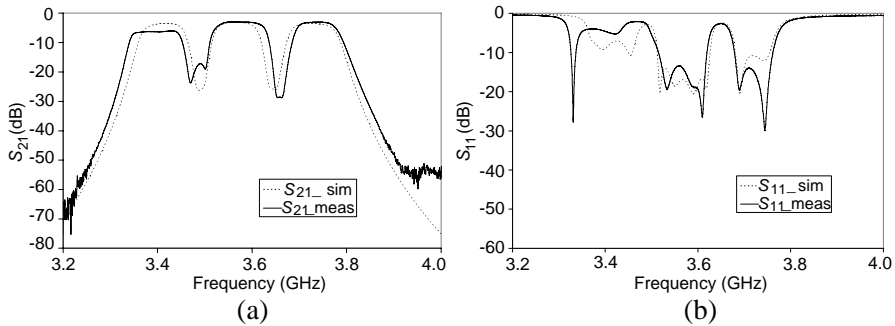


Figure 11. Simulated and measured frequency response of the triple band bandpass filter. (a) S_{21} . (b) S_{11} .

E8363B Network Analyzer. The simulated transmission and reflection characteristics have a very good agreement with the measurement results except in the first band of the filter as shown in Fig. 11. The measured return loss of the triple band bandpass filter is nearly 6 dB in the first passband and 15 dB in the other two passbands. The measured in-band insertion loss is about 5 dB in the first passband and 3.5 dB in the other two passbands. The measured isolation between the two passbands is better than 18 dB. The overall measured bandwidth of this filter is 450 MHz. The size of the filter is 28 mm × 110 mm. One of the possible reasons for these discrepancies is fabrication errors resulting from the over etching of the filter.

Similarly, a quadruple band bandpass filter is realized using open loop resonator. The coupling topology of the quad band bandpass filter is shown in Fig. 12. There are two CQs in the topology for the realization of four transmission zeros. The coupling matrix of the quadruple band bandpass filter is as follows:

$$M = \begin{bmatrix} 0 & 0.7376 & 0 & 0 & 0 & 0 & 0 & 0 & 0 & 0 & 0 & 0 & 0 & 0 & 0 & 0 & 0 & 0 \\ 0.7376 & 0 & 0.7037 & 0 & 0 & 0 & 0 & 0 & 0 & 0 & 0 & 0 & 0 & 0 & 0 & 0 & 0 & 0 \\ 0 & 0.7037 & 0 & 0.4666 & 0 & -0.3654 & 0 & 0 & 0 & 0 & 0 & 0 & 0 & 0 & 0 & 0 & 0 & 0 \\ 0 & 0 & 0.4666 & 0 & 0.4999 & 0 & 0 & 0 & 0 & 0 & 0 & 0 & 0 & 0 & 0 & 0 & 0 & 0 \\ 0 & 0 & 0 & 0.4999 & 0 & 0.2837 & 0 & 0 & 0 & 0 & 0 & 0 & 0 & 0 & 0 & 0 & 0 & 0 \\ 0 & 0 & -0.3654 & 0 & 0.2837 & 0 & 0.7094 & 0 & 0 & 0 & 0 & 0 & 0 & 0 & 0 & 0 & 0 & 0 \\ 0 & 0 & 0 & 0 & 0 & 0 & 0.7094 & 0 & 0.4013 & 0 & 0 & 0 & 0 & 0 & 0 & 0 & 0 & 0 \\ 0 & 0 & 0 & 0 & 0 & 0 & 0 & 0.4013 & 0 & 0.1213 & 0 & -0.4378 & 0 & 0 & 0 & 0 & 0 & 0 \\ 0 & 0 & 0 & 0 & 0 & 0 & 0 & 0 & 0.1213 & 0 & 0.4307 & 0 & 0 & 0 & 0 & 0 & 0 & 0 \\ 0 & 0 & 0 & 0 & 0 & 0 & 0 & 0 & 0 & 0.4307 & 0 & 0.5101 & 0 & 0 & 0 & 0 & 0 & 0 \\ 0 & 0 & 0 & 0 & 0 & 0 & 0 & 0 & -0.4378 & 0 & 0.5101 & 0 & 0.4847 & 0 & 0 & 0 & 0 & 0 \\ 0 & 0 & 0 & 0 & 0 & 0 & 0 & 0 & 0 & 0 & 0 & 0.4847 & 0 & -0.4858 & 0 & 0 & 0 & 0 \\ 0 & 0 & 0 & 0 & 0 & 0 & 0 & 0 & 0 & 0 & 0 & 0 & -0.4858 & 0 & 0.2272 & 0 & 0.4741 & 0 \\ 0 & 0 & 0 & 0 & 0 & 0 & 0 & 0 & 0 & 0 & 0 & 0 & 0 & 0.2272 & 0 & 0.1918 & 0 & 0 \\ 0 & 0 & 0 & 0 & 0 & 0 & 0 & 0 & 0 & 0 & 0 & 0 & 0 & 0 & 0.1918 & 0 & 0.3556 & 0 \\ 0 & 0 & 0 & 0 & 0 & 0 & 0 & 0 & 0 & 0 & 0 & 0 & 0 & 0 & 0 & 0.4741 & 0 & 0.3556 \\ 0 & 0 & 0 & 0 & 0 & 0 & 0 & 0 & 0 & 0 & 0 & 0 & 0 & 0 & 0 & 0 & -0.7037 & 0 \\ 0 & 0 & 0 & 0 & 0 & 0 & 0 & 0 & 0 & 0 & 0 & 0 & 0 & 0 & 0 & 0 & -0.7037 & 0.7376 \\ 0 & 0 & 0 & 0 & 0 & 0 & 0 & 0 & 0 & 0 & 0 & 0 & 0 & 0 & 0 & 0 & 0.7376 & 0 \end{bmatrix}$$

This filter is also fabricated on the RT Duroid 5880 substrate having the dielectric constant of 2.2 and thickness of 0.787 mm. The fabricated quadruple band bandpass filter is shown in Fig. 13(a). The synthesized frequency response of the quad band bandpass filter using the coupling matrix is shown in Fig. 13(b). The simulated and measured frequency responses are in good agreement with each other and they are shown in Fig. 14. The overall size of the filter is 28 mm × 135 mm. The measured insertion loss of the quad band bandpass filter is nearly 5 to 6 dB in each of the passbands. This filter has poor return loss which varies from 5 to 8 dB in each of the passbands. The stopband isolation is better than 20 dB between each of the passbands. The overall measured bandwidth

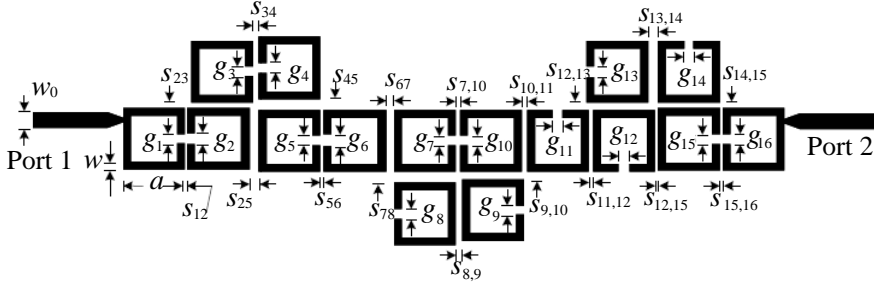
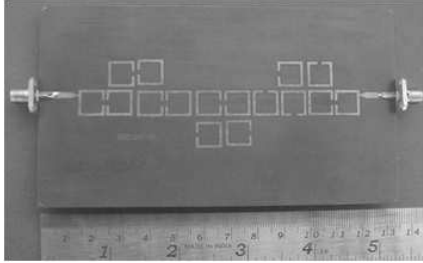
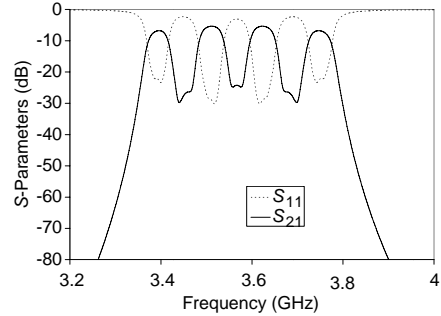


Figure 12. Layout of quadruple band bandpass filter, The physical dimensions of the filter are: $a = 9.71$ mm, $g_1 = 1.38$ mm, $g_2 = 1.73$ mm, $g_3 = 1.56$ mm, $g_4 = 1.56$ mm, $g_5 = 1.56$ mm, $g_6 = 1.91$ mm, $g_7 = 1.56$ mm, $g_8 = 1.56$ mm, $g_9 = 1.39$ mm, $g_{10} = 1.56$ mm, $g_{11} = 1.55$ mm, $g_{12} = 1.73$ mm, $g_{13} = 1.74$ mm, $g_{14} = 1.39$ mm, $g_{15} = 1.56$ mm, $g_{16} = 1.56$ mm, $s_{12} = 0.35$ mm, $s_{23} = 0.89$ mm, $s_{34} = 0.86$ mm, $s_{45} = 1.74$ mm, $s_{56} = 0.52$ mm, $s_{67} = 1.21$ mm, $s_{78} = 1.73$ mm, $s_{89} = 1.04$ mm, $s_{9,10} = 1.22$ mm, $s_{10,11} = 0.87$ mm, $s_{11,12} = 0.69$ mm, $s_{12,13} = 1.22$ mm, $s_{13,14} = 1.56$ mm, $s_{14,15} = 0.87$ mm, $s_{15,16} = 0.52$ mm, $s_{25} = 1.39$ mm, $s_{7,10} = 0.69$ mm, $s_{12,15} = 0.52$ mm.



(a)



(b)

Figure 13. (a) Fabricated quadruple band bandpass filter. (b) Synthesized frequency response of quadruple band bandpass filter considering the finite Q -factor of the resonator $Q = 240$.

in this filter is about 410 MHz. The asymmetry in the filter response may be due to the limitation of proposed theory which is valid for the narrow band filter.

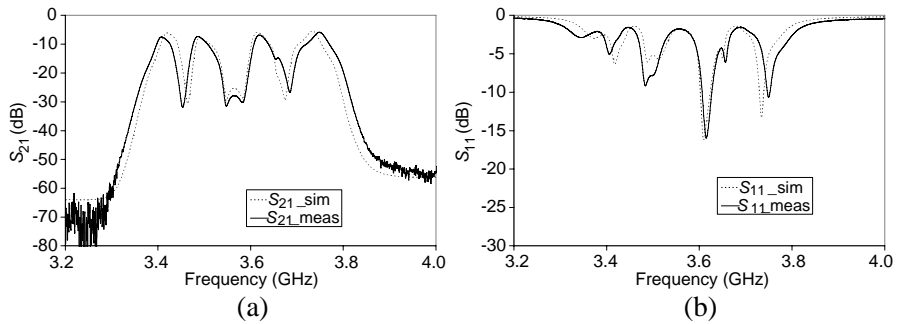


Figure 14. Simulated and measured frequency response of the quadruple band bandpass filter. (a) S_{21} . (b) S_{11} .

6. CONCLUSION

A generalized synthesis of symmetrical multiple passband filters is presented in this paper. This synthesis is based on the frequency transformation method. It can be used for the multiple passband filters having any number of passbands. Using this frequency transformation, the poles and zeros of the multiband filtering function have been derived. The coupling matrix is derived from the poles and zeros of the multiband filtering function. A couple of filters having different number of passband have been synthesized using the coupling matrix in order to validate the present approach of the multiband filter synthesis. Two multiple band bandpass filters have been synthesized, designed, fabricated and tested to validate the multiple passband filter synthesis. These frequency response of the fabricated filters has good agreement with simulated results.

Our main aim in this paper is to present the generalized frequency transformation technique for the synthesis of multiband filter. The new technique is proposed in order to replace the conventional optimization method. The theory of symmetric multiple band bandpass can be further modified and extended to asymmetric multiple band bandpass filters.

ACKNOWLEDGMENT

The authors thank to the PCB fabrication facility of Space Applications Center, Indian Space Research Organisation, Ahmedabad, India for the fabrication of the filters.

REFERENCES

1. Holme, S., "Multiple passband filters for satellite applications," *Proc. 20th AIAA Int. Communications Satellite Systems Conf. Exhibit*, 2002.
2. Lee, J., M. S. Uhm, and I.-B. Yom, "A dual-passband filter of canonical structure for satellite applications," *IEEE Microwave and Wireless Components Letters*, Vol. 14, 271–273, 2004.
3. Jachowski, D. R., "Folded multiple bandpass filter with various couplings," US Patent 5410284, 1995.
4. Wu, M. S., Y. Z. Chueh, J. C. Yeh, and S. G. Mao, "Synthesis of triple-band and quad-band bandpass filters using lumped-element coplanar waveguide resonators," *Progress In Electromagnetics Research B*, 433–451, 2009.
5. Mokhtaari, M., J. Bornemann, K. Rambabu, and S. Amari, "Coupling-matrix design of dual and triple passband filters," *IEEE Transactions on Microwave Theory and Techniques*, Vol. 54, 3940–3946, 2006.
6. Chiou, Y. C. and J. T. Kuo, "Planar multiband bandpass filter with multimode stepped-impedance resonators," *Progress In Electromagnetics Research*, Vol. 114, 129–144, 2011.
7. Yunchi, Z., K. A. Zaki, J. A. Ruiz-Cruz, and A. E. Atia, "Analytical synthesis of generalized multi-band microwave filters," in *2007 IEEE/MTT-S International Microwave Symposium*, 1273–1276, 2007.
8. Lunot, V., F. Seyfert, S. Bila, and A. Nasser, "Certified computation of optimal multiband filtering functions," *IEEE Transactions on Microwave Theory and Techniques*, Vol. 56, 105–112, 2008.
9. Macchiarella, G. and S. Tamiazzo, "Design techniques for dual-passband filters," *IEEE Transactions on Microwave Theory and Techniques*, Vol. 53, 3265–3271, 2005.
10. Juseop, L. and K. Sarabandi, "A synthesis method for dual-passband microwave filters," *IEEE Transactions on Microwave Theory and Techniques*, Vol. 55, 1163–1170, 2007.
11. Juseop, L. and K. Sarabandi, "Design of triple-passband microwave filters using frequency transformations," *IEEE Transactions on Microwave Theory and Techniques*, Vol. 56, 187–193, 2008.
12. Kuo, Y.-T., J.-C. Lu, C.-K. Liao, and C.-Y. Chang, "New multiband coupling matrix synthesis technique and its microstrip implementation," *IEEE Transactions on Microwave Theory and*

- Techniques*, Vol. 58, 1840–1850, 2010.
13. Garcia-Lamperez, A. and M. Salazar-Palma, “Single-band to multiband frequency transformation for multiband filters,” *IEEE Transactions on Microwave Theory and Techniques*, Vol. 59, 3048–3058, 2011.
 14. Cameron, R. J., “Advanced coupling matrix synthesis techniques for microwave filters,” *IEEE Transactions on Microwave Theory and Techniques*, Vol. 51, 1–10, 2003.
 15. Bell, Jr., H. C., “Canonical asymmetric coupled-resonator filters,” *IEEE Transactions on Microwave Theory and Techniques*, Vol. 30, 1335–1340, 1982.
 16. Juseop, L. and K. Sarabandi, “Synthesizing microwave resonator filters,” *IEEE Microwave Magazine*, Vol. 10, 57–65, 2009.
 17. Tamiazzo, S. and G. Macchiarella, “An analytical technique for the synthesis of cascaded N -tuplets cross-coupled resonators microwave filters using matrix rotations,” *IEEE Transactions on Microwave Theory and Techniques*, Vol. 53, 1693–1698, 2005.
 18. Cameron, R. J., “General coupling matrix synthesis methods for Chebyshev filtering functions,” *IEEE Transactions on Microwave Theory and Techniques*, Vol. 47, 433–442, 1999.
 19. Ness, J. B., “A unified approach to the design, measurement, and tuning of coupled-resonator filters,” *IEEE Transactions on Microwave Theory and Techniques*, Vol. 46, 343–351, 1998.
 20. Hong, J.-S. and M. J. Lancaster, “Couplings of microstrip square open-loop resonators for cross-coupled planar microwave filters,” *IEEE Transactions on Microwave Theory and Techniques*, Vol. 44, 2099–2109, 1996.